NANOMEDICINE AND NANOTECHNOLOGY JOURNAL Open Access

SCIENTIFIC LITERATURE

SHORT COMMUNICATION

Enhanced Stability of Hepatitis E Virus Nanoparticles via Au-Nanocluster Surface Modulation

Mo A. Baikoghli, Chun-Chieh Chen, Michelle Nguyen and R Holland Cheng*

Department of Molecular and Cellular Biology, University of California, USA

ARTICLE INFO

Article history:
Received: 14 May 2018
Accepted: 06 June 2018
Published: 07 June 2018

Keywords:
Hepatitis e nanoparticle;
HEVNP;
Chemical surface modulation;
Cancer diagnosis;
Site-specific delivery;
Non-invasive delivery;
Gold-nanoclusters;
Au102 pMBA;
HEVNP+Au102C6MI;
Hyperthermia treatment;
Hevvlp;
Virus-like particles

Citation this article: Baikoghli MA, Chen CC, Nguyen M, Cheng RH. Enhanced Stability of Hepatitis E Virus Nanoparticles via Au-Nanocluster Surface Modulation. NanomedNanotechnol J. 2018; 2(1):116.

Correspondence:
R Holland Cheng,
Department of Molecular and Cellular Biology, University of California, Davis, CA, USA,
Tel: (530) 988-8459;
Email: rhch@ucdavis.edu

ABSTRACT

The technological advances in fields of nanomedicine and nanotechnology have allowed for the design and development of some of the most sophisticated nanoparticle systems. Among which, protein-based nanocapsids have gained tremendous attention as nanoplatform systems for delivery of theranostic agents due to their low toxicity and high bioavailability. Here we describe the enhanced stability of hepatitis E nanoparticles (HEVNP) that is facilitated by gold-nanocluster surface conjugation.

Abbreviations

VLP: Virus-Like Particles; HEVNP: Hepatitis E virus nanoparticle; FDA: US Federal Food and Drug Administration; HBV: Hepatitis B Virus; HEV: Hepatitis E Virus; HIV: Human Immunodeficiency Virus; NP: Nanoparticles; HPV: Human Papillomavirus; ORF2: Open Reading Frame 2; pMBA: p-mercaptobenzoic acid; GI: Gastrointestinal; Kb: Kilobase; AuNC: Gold (Au) NanoClusters; AA: Amino Acids; SPR: Single Particle Reconstruction; PFT: Polar Fourier Transformation

Introduction

The use of nanoparticles has been a central focus in nanotechnology and nanomedicine; this technology offers promising approaches to diagnosis, targeting, and treatment[1, 2]. Traditional approaches to battle cancer commonly involve surgery, chemotherapy, and radiation[3]. While these methods are somewhat effective in diagnosis and treatment of cancerous regions, the lack of specificity in targeting hampers the efficiency of treatment and causes damage to healthy cells.

Among nanoparticulate systems such as polymer-based, lipid-based, or dendrimers, a handful of protein-based capsids, derived from viruses, also known as virus-like particles (VLPs), have the lowest toxicity levels and highest bioavailability [4]. To date, several prophylactic VLPs have been approved by the FDA as commercialized vaccines. These include GlaxoSmithKline's Engerix® (hepatitis B virus) and Cervarix® (human papillomavirus), and Merck and Co., Inc.'s Recombivax HB® (hepatitis B virus) and Gardasil® (human papillomavirus) [5]. Other VLP-based vaccines are currently under clinical development against influenza, parvovirus, and Norwalk virus [5,6]. The advances in VLP technology is not limited to vaccination; VLPs are also

also ideal candidates as drug carriers due to their high bioavailability [7,8]. Recent advances in chemical surface modulation has promoted VLPs into capable multi-modality vehicles for antigen delivery, targeting ligand, and tracking molecules[9-12].

Hepatitis E nanoparticles (HEVNPs) have shown great promise in nucleic acid, and metabolic drug encapsulation, as well as surface modulation[11, 13]. Since HEV naturally infects via feco-oral routes, the HEV protein capsid has gained the evolutionary advantage to survive the harsh acidic and enzymatic conditions of the GI tract, and therefore, the non-infectious nanoparticles derived from HEV can be readily utilized for oral and mucosal administration [14-17]. The technological achievements of HEVNP are summarized in review articles by Baikoghli et al. 2018 and Stark et al. 2016[13]. Here we highlight and discuss the surface modulation of HEVNP in the context of tracking molecule surface modulation via AuNCs, and overall stability of the nanoparticle under two different pH conditions.

Hepatitis E Virus Nanoparticles

Hepatitis E virus (HEV) is a positive sense single stranded RNA virus, with genome size of 7.2 kb and a diameter of 320–340 Å. Genetic modifications to the ORF2 of HEV, including 111AA truncation to the N-terminus and 52 AA truncation to the C-terminus, results in the formation of smaller, genome-freeHEV nanoparticles with a diameter of 250-270 Å[18, 19]. The structure of HEVNP has been resolved by x-ray crystallography [20]. HEVNP retains the icosahedral stability of the virion when producedby baculovirus expression vector system [19, 21]. There are sixty subunits, composed of three domainseach, forming the icosahedral capsid of HEVNP (Figure 1 A). The shell domain (S) (AA: 118-317) is critical in inter-subunit interactions, stabilizing the icosahedral capsid. The middle domain (M) (AA: 318-451) binds and interacts with the S domain[11, 22]. The protrusion domain (P) (452-606) forms a dimeric spike at the 2-fold axis. The M domain is connected to the P domain via a proline-rich hinge, which facilitates the topological changes in the protruding spikes[19, 21].

The surface of HEVNPis composed of multiple anchoring sites that arerepeated in the sixty identical subunits which can be modulated with various conjugates. Such modularity allows for easy conjugation of small peptides, tissue-targeting molecules, and tracking molecules such as fluorescent dye and gold nanoclusters. Moreover, in the bottom of the shell (S) domain, positively charged residues at the N-terminus, facing the interior surface of HEVNP, can be used for encapsulation of DNA, CRISPR RNA, and proteins. Exposed P domain loops(loops I (483-491), II (530-535), III (554-561), IV (582-593), and 573C) can function as targeting-ligand conjugation sites[11, 23].The P domain of HEVNP surface is composed of multiple anchoring sites in each of the sixty identical subunits, which can be used for surface functionalization, without altering the icosahedral organization of the capsid protein[11, 15].

HEVNP Surface Modulation

Surface functionalization of nanoparticles is a critical step towards selective conjugation of naturally occurring and synthetic molecules. In 2013, Jariyapong et al. genetically inserted a highly immunogenic 15 residue peptide (p18), derived from the third hypervariable loop of HIV onto the surface of HEVNP[15]. Displaying 60 copies of p18, the chimeric HEVNP triggered a robust HIV-1-specific CTL response. The insertion, after the residue Tyr485 did not interfere with the icosahedral arrangement and overall stability of HEVNP. While this has proven to be a highly effective approach for mucosal vaccination, the conjugation method had its limitations; including repeatability and highly labor intensive chimeric-HEVNP production[11, 13, 15].

In 2016, Chen and colleagues, utilized a thiol-ligand exchange approach to functionalize the surface of HEVNP. For surface conjugation on P domain, 5 cysteine replacement sites were selected; these include Y485, T489, Y533, N573, and T586. Of the five engineered sites, N573C was best suited for further modification. To this end, a breast cancer targeting ligand, LXY30[24] was conjugated to the N573C site. As a proof of concept, in vivo studies carried out in mice showed that HEVNPs without LXY30 do not accumulate at the tumor

site, but LXY30 functionalized HEVNPs do. Compared to genetic modifications, chemical conjugation is a more efficient and highly reproducible method for surface functionalization[11].

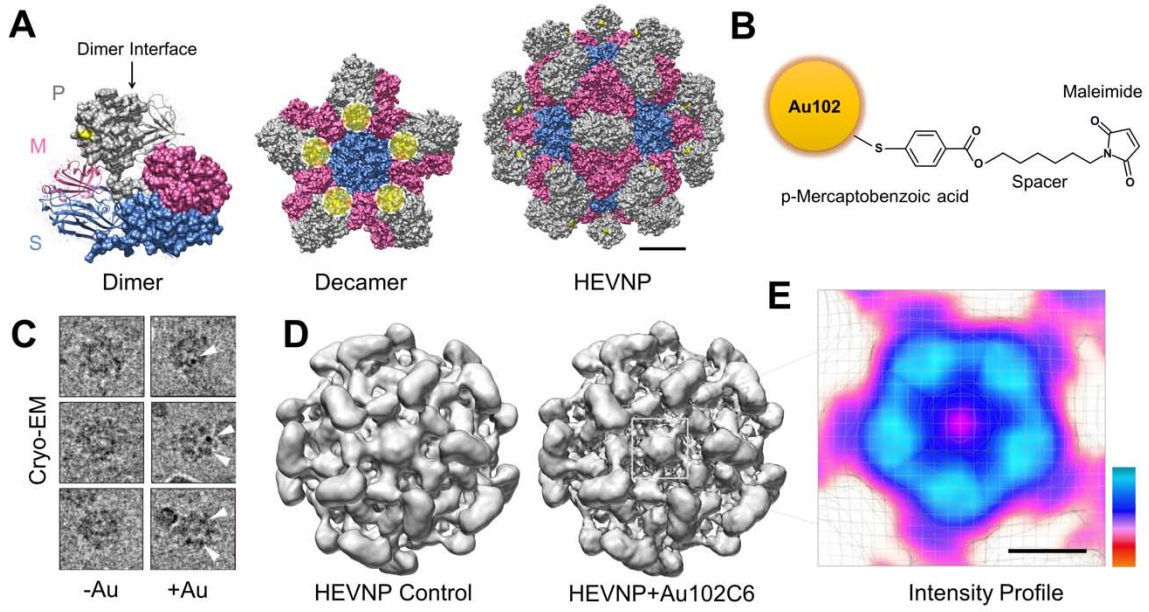

Figure 1. Surface functionalization of HEVNP with AuNC.(A) Capsid protein composition of HEVNP includes dimeric subunits comprised of shell (s), middle (m), and protrusion (p) domains. P-domain is stabilized with a proline-rich hinge connected to the M-domain, while the S domain stabilized the icosahedral shell. The P-domain is utilized for surface functionalization. Here, residue 573 (highlighted in yellow) was replaced with a cysteine to allow for thiol-exchange disulfide bonding. The dimers form pentamers (thus decamers), stabilized by local intermolecular interactions at the 5-fold axis, and assemble into capsid shell of HEVNP via Ca+ bridges at the 3-fold. **(B)** Au102-pMBA-C6-Maleimide (AuNC) is conjugated to the 573C through thiol-exchange reaction. **(C)** Cryo-Electron Microscopy was employed to characterize the AuNC and to process data for 3D reconstruction through single particle analysis. Comparison between Au-free HEVNP and Au-conjugated HEVNP is characterized by high intensity regions pointed by the arrows. **(D)** Resulting 3D reconstructions with HEVNP as control and HEVNP+Au102C6, show high intensity regions around 5-fold axis **(E)**, suggesting AuNC localization and stabilization around the 5-fold axis.

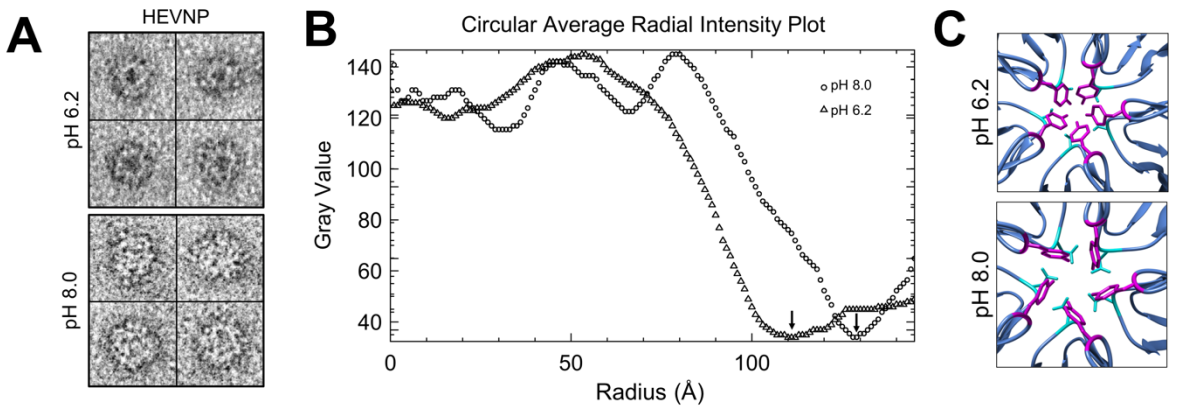

Figure 2. Stability of HEVNP is reduced at high pH as a result of weakened intermolecular interactions at the 5-fold interface.(A) TEM images of HEVNP at pH 6.2 and pH 8.0; showing larger particles at pH 8.0. (B) Circular averaging and 1-D intensity profiling. HEVNP at pH 8.0 were about 10-15% larger than HEVNP without AuNC. (C) Molecular modeling indicated that intermolecular interactions were reduced at the 5-fold as pH is increased to 8.

Co-localization of AuNCs around the icosahedral 5-Fold Axis of HEVNP

Recently, Stark and colleagues successfully conjugated magnetic nano-gold clusters, functionalized with pMBA44, a six carbon long spacer, and maleimide linker, (HEVNP+Au102C6MI from hereafter) to the 573C site on HEVNP (Figure 1 A & B)[25-27]. The structure, surface charge, and electronic and vibrational characteristics of Au102 have been extensively described [26, 28-30]. The HEVNP+Au102C6MIwere purified and prepared for cryo-EM analysis. A comparative 2D analysis was carried out and unique, electron-dense regions that were observed in the Au102C6MIconjugated HEVNPs (Figure 1 C). Cryo-EM single particle analysis was carried out to achieve a 3D density map of the functionalized nanoparticles, as well as 573C-HEVNPs as control. From the collected datasets, a three-dimensionalinitial model was generated through an iterative de novo approach to determine and cross-validate particle parameters[31]. A robust PFT-based particle screening protocol was employed to determine particle orientation with respect to three angles phi, theta, and omega, as well as Cartesian coordinates[32, 33]. Furthermore, using scale factor analysis integrated in the PFT package, the particles were screened to reduce size heterogeneity[32]. Subsequently, 3D reconstruction and refinement was carried out (Figure 1 D)[31, 34].

For validation and structural analysis via difference mapping, we carried out simultaneous 3D reconstruction on both control and HEVNP+Au102C6MI. In both reconstructs, the S, M, and P domains were clearly resolved (Figure 1D). In addition, 2D and 3D image analysis of HEVNP+Au102C6MIrevealed five unique high-density regionsthat were present around the 5-fold axis in a doughnut-like array, and not present in the control reconstruction; validated by difference mapping[25]. Local intensity analysis was performed to characterize the HEVNP+Au102C6MI 5-fold axis densities to confirm the size of Au102C6MI. It was shown that the addition of the C6 linker arm to the Au102 pMBA provides support for the doughnut-like colocalization to stabilize around the 5-fold axis of HEVNP (Figure 1 E). We hypothesize that such co-localization around the 5-fold axis of HEVNP may enhance the stability of the nanoparticle by increasing the stability of intramolecular interactions, supporting the decametric interface.

Impact of pH on the Stability of HEVNP

The highly compact intermolecular interface at the icosahedral 5-fold axis iscritical for nanocapsid assembly and stability. Comprised of residues only in the S domain, the decametric interactions at the 5-fold axis are tighter than those at the dimer and trimers at the 2-fold and 3-fold axes, respectively. There are 4 loops between the beta-sheets in the S domain; 2 out of the 4 loops are involved in inter-molecular interactions with adjacent subunits. These interactions are mediated by side chains of Asn-200 and Tyr-288, which are separated by a distance of less than5 Angstroms[23, 35]. Site-mutation studies have revealed that these residues are critical for nanocapsid formation and stability. It is noteworthy to mention that similar 5-fold interactions mediated by aromatic amino acids such as Phe and Tyr are also observed in rNV(Recombinant Norwalk Virus), SMSV (San Miguel Sea Lion Virus), and CARMV (Carnation Mottle Virus); suggesting an evolutionary significance of the 5-fold intermolecular interface in nanocapsid formation[23].

To test whether the enhanced stability of HEVNP via Au102C6MIis facilitated by colocalization around the 5-fold icosahedral axis, we carried out pH stability experiments. It was previously reported that HEVNP is most stable at pH 6.2; at this optimal pH, the Ca+ bridge at the 3-fold axis and the intermolecular interactions at the 5-fold axis provide stability to the T=1 icosahedral protein capsid. At pH 8.0, HEVNP begins to swell, suggesting weakened intermolecular interfaces enforcingthe compact T=1 icosahedral conformation. We carried out pH stability experimentation by incubating the HEVNPs in pH 6.2 and pH 8.0 buffers overnight. TEM imaging revealed a significant difference in size for the HEVNP nanoparticles in pH 6.2 (average diameter 23 nm), and pH 8.0

(average diameter 27 nm) (Figure 2 A). To quantitatively describe our TEM observational analysis, the particles were subject to circular averaging in order to map out radial intensity analysis (Figure 2 B). It was observed that particles at pH 8.0 are on average 10-15% larger than those at pH 6.2. Furthermore, molecular modeling was carried out to observe intermolecular interactions at the 5-fold axis under pH 6.2 and pH 8.0; the results suggest a weaker interface at pH 8.0 (Figure 2 C). These results indicate that at pH 8.0, the HEVNP particles may have collapsed or the capsid protein stability is significantly weakened.

We hypothesize that structural preservation of the 5-fold intermolecular interface may play a critical role in the enhancement of HEVNP's stability at higher pH levels. After the HEVNP+Au102C6MIwere incubated in pH 6.2 and pH 8.0 buffers overnight, TEM imaging revealed that the Au102C6MIconjugated HEVNPs did not increase in capsid size as a consequence of a weakened stability due to the relaxed interactions between the capsid subunits (Figure 3 A). Similarly, we carried out 2D circular averaging of the capsid projections to comparatively study the radial intensity profile of these particles. Unlike the control capsid without gold conjugates, we observed no significant changes of the capsid projection in radius (Figure 3 B). These results indicate that the co-localization of the Au102C6MIaround the 5-fold axis may reinforce intermolecular interactions at the S domain interface, and thus enhance the stability of HEVNPs at higher pH values.

Conclusion

Previously, cryo-EM SPR revealed that the Au102C6MI surface conjugation results in theformation of a doughnut-like ring around the 5-fold icosahedral axis of HEVNP[25]. The Au102 core is measured to be 1.5 nm, while the hydrodynamic diameter (including pMBA) measures to be about 2.5 nm. These dimensions fit well with the densities observed in the cryo-EM 3D reconstruction density map of HEVNP+Au102C6MI. The C6spacer is about 1.1nm, so the distance from the center of the gold core to the maleimide binding site (573C) is approximately 2-3 nm, all together. The length of the C6 arms is sufficient to provide enough flexibility for Au102C6MIcolocalize aroundthe 5-fold axis (Figure 3 C-E). Here, we demonstrated that the conjugation of Au102C6MIenhances the overall stability of HEVNP at pH 8.0; whereas the control HEVNP particles show an increase in overall size, and weakened compactness at pH 8.0.

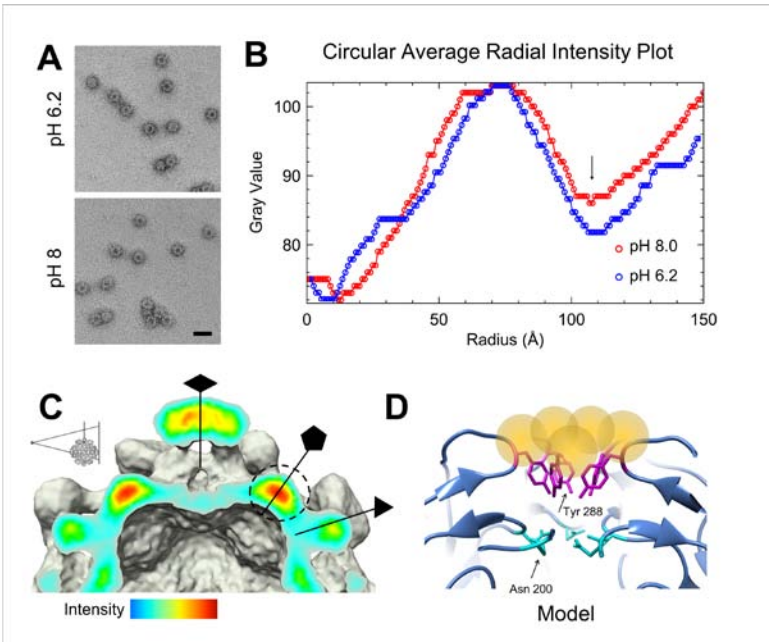

Figure 3. Enhanced stability of HEVNP after AuNC-C6 conjugation. **(A)** TEM images of HEVNP conjugated to AuNC-C6 revealed that the overall size of the HEVNP does not change with increased pH. **(B)** Circular averaging and 1-D intensity profiling. No changes to the HEVNP size as a result of increased pH. **(C)** 2D intensity slice cross-section analysis revealed high intensity regions at the 5-fold of the cryo-EM reconstructed 3D density map was observed. **(D)** A model showing the mechanism by which critical intermolecular interactions are potentially preserved by colocalization of AuNC-C6 around the icosahedral 5-fold axis of HEVNP.

The trend towards the usage of nanoparticulate systems has gravitated tremendous attention in the nanomedicine field. The composition and reproducibility of nanoparticle systems is critical in the context of nanodelivery systems. Furthermore, the effectiveness of nanoparticle systems in nanomedicine is governed by bioavailability and compatibility with physiological conditions. As such, hepatitis E nanoparticles have shown considerable potential in encapsulation of nanotheranostics and surface modulation. The applications of such protein-based platform ranges from tissue-specific delivery of drugs, nucleic acids, and inorganic metals, to surface modulation for mucosal vaccination, cancer theranostics, and particle tracking.

The enhanced stability of HEVNP demonstrated in this reportcan be beneficial towards particle tracking studies. While, highly sensitive fluorescence microscopy techniques allow single nanoparticle tracking during the uptake into living cells [37], a higher spatial resolution in the sub-nm range can be achieved by TEM. Utilizing theuniform electron dense Au102C6MI[27, 38], electron microscopic studies can be carried out to further our understanding of the distribution of particles in targeted tissues and their specific interactions with cells; cryo-fixation and chemical fixation techniques can be employed to process tissues in resin blocks and subsequently sectioned by ultramicrotomy for 2D and 3D studies by transmission electron microscopy[39, 40].

In the context of tumor-targeted hyperthermia treatment, enhanced stability of HEVNP via Au102C6MI-conjugation may serve as an advantage in electromagnetic field enhancement of the radiative properties of Au102[41]. It has been reported that strong local surface plasmon resonance develops in AuNC protected by thiolate monolayer[42]. Moreover, if the Au nanoparticles are small enough (ranging between 1.5 – 3.0 nm in diameter), strong plasmon resonance occurs with the gold at wavelengths ranging between 520-540 nm[42, 43]. Laser-induced tissue hyperthermia has proven to be effective in cancer phototherapy[44], and the tissue-specific targeting of cancer and tumors via multimodal HEVNPs can enhance the accuracy of targeting and efficacy during treatment.

Acknowledgements

We acknowledge funding support to Professor Holland Cheng by NIH grant numbers: A1095382, EB021230, CA198880, National Institute of Food and Agriculture, as well as Finland Distinguished Professor Program.

The authors wish to express gratitude to Marie Stark, Li Xing, and Prasida Holla for their early contribution in the material preparation towards data analysis, similarly to Aria Sikaroudi, Marina Nguyen, and Juliana Noronha for sample/data processing. We acknowledge George Kamita for manuscript composition, and Hannu Häkkinen and Varpu Marjomäki for the stimulating discussions.

References

1. Zhang L, Gu FX, Chan JM, Wang AZ, Langer RS, et al. (2008). Nanoparticles in medicine: therapeutic applications and developments. Clinical pharmacology & therapeutics. 83: 761-769.

2. Zhao L, Seth A, Wibowo N, Zhao CX, Mitter N, et al. (2014). Nanoparticle vaccines. Vaccine. 32: 327-337.

3. Choi KY, Liu G, Lee S, Chen X. (2012). Theranostic nanoplatforms for simultaneous cancer imaging and therapy: current approaches and future perspectives. Nanoscale. 4: 330-342.

4. Yildiz I, Shukla S, Steinmetz NF. (2011). Applications of viral nanoparticles in medicine. Current opinion in biotechnology. 22: 901-908.

5. Roldão A, Mellado MC, Castilho LR, Carrondo MJ, Alves PM. (2010). Virus-like particles in vaccine development. Expert review of vaccines. 9: 1149-1176.

6. Pinto LA, Edwards J, Castle PE, Harro CD, Lowy DR, et al. (2003). Cellular immune responses to human papillomavirus (HPV)-16 L1 in healthy volunteers immunized with recombinant HPV-16 L1 virus-like particles. The Journal of infectious diseases. 188: 327-338.

7. Ma Y, Nolte RJ, Cornelissen JJ. (2012). Virus-based nanocarriers for drug delivery. Advanced drug delivery reviews. 64: 811-825.

8. Molino NM, Wang SW. (2014). Caged protein nanoparticles for drug delivery. Current opinion in biotechnology. 28: 75-82.

9. Garcea RL, Gissmann L. (2004). Virus-like particles as vaccines and vessels for the delivery of small molecules. Current opinion in biotechnology. 15: 513-517.

10. Schoonen L, van Hest JC. (2014). Functionalization of protein-based nanocages for drug delivery applications. Nanoscale. 6: 7124-7141.

11. Chen CC, Xing L, Stark M, Ou T, Holla P, et al. (2016). Chemically activatable viral capsid functionalized for cancer targeting. Nanomedicine. 11: 377-390.

12. Chun-Chieh Chen, Marie Stark, Mo A Baikoghli, R Holland Cheng. (2017). Hepatitis E Virus Nanoparticle Encapsulating Nano-Theranostic Reagent as Modularized Capsule. 5: 1-4.

13. Stark M, Cheng RH. (2016). Surface modulatable nanocapsids for targeting and tracking toward nanotheranostic delivery. Pharmaceutical patent analyst. 5: 307-317.

14. Takamura S, Niikura M, Li TC, Takeda N, Kusagawa S, et al. (2004). DNA vaccine-encapsulated virus-like particles derived from an orally transmissible virus stimulate mucosal and systemic immune responses by oral administration. Gene therapy. 11: 628-635.

15. Jariyapong P, Xing L, van Houten NE, Li TC, Weerachatyanukul W, et al. (2013). Chimeric hepatitis E virus-like particle as a carrier for oral-delivery. Vaccine. 31: 417-424.

16. P Holla, MA Baikoghli, P Soonsawad, RH Cheng. (2017). Toward Mucosal DNA Delivery: Structural Modularity in Vaccine Platform Design, in Micro and Nanotechnology in Vaccine Development. Elsevier. 303-326.

17. Chen CC, Baikoghli MA, Cheng RH. (2018). Tissue targeted nanocapsids for oral insulin delivery via drink. Future Science.

18. Xing L, Kato K, Li T, Takeda N, Miyamura T, et al. (1999). Recombinant hepatitis E capsid protein self-assembles into a dual-domain T= 1 particle presenting native virus epitopes. Virology. 265: 35-45.

19. Xing L, Li TC, Mayazaki N, Simon MN, Wall JS, et al. (2010). Structure of hepatitis E virion-sized particle reveals an RNA-dependent viral assembly pathway. Journal of Biological Chemistry. 285: 33175-33183.

20. Xing L, oseph C Wang, Tian-Cheng Li, Yasuhiro Yasutomi, James Lara, et al. (2011). Spatial configuration of hepatitis E virus antigenic domain. Journal of virology. 85: 1117-1124.

21. Li TC, Takeda N, Miyamura T, Matsuura Y, Wang JC, et al. (2005). Essential elements of the capsid protein for self-assembly into empty virus-like particles of hepatitis E virus. Journal of virology. 79: 12999-13006.

22. Mori Y, Matsuura Y. (2011). Structure of hepatitis E viral particle. Virus research. 161: 59-64.

23. Yamashita T, Mori Y, Miyazaki N, Cheng RH, Yoshimura M, et al. (2009). Biological and immunological characteristics of hepatitis E virus-like particles based on the crystal structure. Proceedings of the National Academy of Sciences. 106: 12986-12991.

24. Xiao W, Tianhong Li, Fernanda C Bononi, Diana Lac, Ivy A Kekessie, et al. (2016). Discovery and characterization of a high-affinity and high-specificity peptide ligand LXY30 for in vivo targeting of α3 integrin-expressing human tumors. EJNMMI research. 6: 18.

25. Stark MC, Baikoghli MA, Lahtinen T, Malola S, Xing L, et al. (2017). Structural characterization of site-modified nanocapsid with monodispersed gold clusters. Scientific reports. 7: 17048.

26. Koivisto J, Xi Chen, Serena Donnini, Tanja Lahtinen, Hannu Häkkinen, et al. (2016). Acid–Base Properties and Surface Charge Distribution of the Water-Soluble Au_{102} (p MBA)$_{44}$ Nanocluster. The Journal of Physical Chemistry C. 120: 10041-10050.

27. Lahtinen T, Lahtinen T, Haataja JS, Tero TR, Häkkinen H, et al. (2016). Template-Free Supracolloidal Self-Assembly of Atomically Precise Gold Nanoclusters: From 2D Colloidal Crystals to Spherical Capsids. Angewandte Chemie International Edition. 55: 16035-16038.

28. Hulkko E, Olga Lopez-Acevedo, Jaakko Koivisto, Yael Levi-Kalisman, Roger D Kornberg, et al. (2011). Electronic and Vibrational Signatures of the

Au_{102} (p-MBA)$_{44}$ Cluster. Journal of the American Chemical Society. 133: 3752-3755.

29. Jadzinsky PD, Calero G, Ackerson CJ, Bushnell DA, Kornberg RD. (2007). Structure of a thiol monolayer-protected gold nanoparticle at 1.1 Å resolution. Science. 318: 430-433.

30. Salorinne K, Sami Malola, O Andrea Wong, Christopher D Rithner, Xi Chen, et al. (2016). Conformation and dynamics of the ligand shell of a water-soluble Au_{102} nanoparticle. Nature communications. 7: 10401.

31. Guo F, Jiang W. (2014). Single particle cryo-electron microscopy and 3-D reconstruction of viruses. in Electron Microscopy. Springer. 401-443.

32. Baker TS, Cheng RH. (1996). A model-based approach for determining orientations of biological macromolecules imaged by cryoelectron microscopy. Journal of structural biology. 116: 120-130.

33. Acar E, Mo A Baikoghli, Marie Stark, Sari Peltonen, Ulla Ruotsalainen, et al. (2017). Multiresolution MAPEM Method for 3D Reconstruction of Symmetrical Particles with Electron Microscopy. EMBEC & NBC 2017. Springer. 141-144.

34. Ludtke SJ, Baldwin PR, Chiu W. (1999). EMAN: semiautomated software for high-resolution single-particle reconstructions. Journal of structural biology. 128: 82-97.

35. Li TC, Yamakawa Y, Suzuki K, Tatsumi M, Razak MA, et al. (1997). Expression and self-assembly of empty virus-like particles of hepatitis E virus. Journal of virology. 71: 7207-7213.

36. Schindelin J, Arganda-Carreras I, Frise E, Kaynig V, Longair M, et al. (2012). Fiji: an open-source platform for biological-image analysis. Nature methods. 9: 676-682.

37. Ruthardt N, Lamb DC, Bräuchle C. (2011). Single-particle tracking as a quantitative microscopy-based approach to unravel cell entry mechanisms of viruses and pharmaceutical nanoparticles. Molecular therapy. 19: 1199-1211.

38. Salorinne K, Tanja Lahtinen, Sami Malola, Jaakko Koivisto, Hannu Häkkinen. (2014). Solvation chemistry of water-soluble thiol-protected gold nanocluster Au_{102} from DOSY NMR spectroscopy and DFT calculations. Nanoscale. 6: 7823-7826.

39. Paavolainen L, Erman Acar, Uygar Tuna, Sari Peltonen, Toshio Moriya, et al. (2014). Compensation of missing wedge effects with sequential statistical reconstruction in electron tomography. PloS one. 9: e108978.

40. Pan Soonsawad, Li Xing, Emerson Milla, Juan M Espinoza, Masaaki Kawano, et al. (2010). Structural evidence of glycoprotein assembly in cellular membrane compartments prior to Alphavirus budding. Journal of virology. 84: 11145-11151.

41. Eustis S, MA El-Sayed. (2006). Why gold nanoparticles are more precious than pretty gold: noble metal surface plasmon resonance and its enhancement of the radiative and nonradiative properties of nanocrystals of different shapes. Chemical society reviews. 35: 209-217.

42. Malola S, Lehtovaara L, Enkovaara J, Häkkinen H. (2013). Birth of the localized surface plasmon resonance in monolayer-protected gold nanoclusters. Acs Nano. 7: 10263-10270.

43. Ghosh SK, T Pal. (2007). Interparticle coupling effect on the surface plasmon resonance of gold nanoparticles: from theory to applications. Chemical reviews. 107: 4797-4862.

44. Terentyuk GS, Maslyakova GN, Suleymanova LV, Khlebtsov NG, Khlebtsov BN, et al. (2009). Laser-induced tissue hyperthermia mediated by gold nanoparticles: toward cancer phototherapy. Journal of biomedical optics. 14: 021016.